THE JOURNAL OF BIOLOGICAL CHEMISTRY VOL. 288, NO. 49, pp. 35081–35092, December 6, 2013
© 2013 by The American Society for Biochemistry and Molecular Biology, Inc. Published in the U.S.A.

Silencing of the Tandem Pore Domain Halothane-inhibited K^+ Channel 2 (THIK2) Relies on Combined Intracellular Retention and Low Intrinsic Activity at the Plasma Membrane*[S]

Received for publication, July 19, 2013, and in revised form, October 24, 2013 Published, JBC Papers in Press, October 25, 2013, DOI 10.1074/jbc.M113.503318

Franck C. Chatelain[1], Delphine Bichet[1], Sylvain Feliciangeli, Marie-Madeleine Larroque, Véronique M. Braud, Dominique Douguet, and Florian Lesage[2]

From the Laboratory of Excellence Ion Channel Science and Therapeutics, Institut de Pharmacologie Moléculaire et Cellulaire, CNRS, and Université de Nice Sophia Antipolis, 660 Route des Lucioles, 06560 Valbonne, France

Background: THIK2 does not generate macroscopic currents in heterologous systems.
Results: THIK2 produces K^+ currents when mutated in its pore region and/or in its cytoplasmic amino terminus.
Conclusion: Silencing of THIK2 is due to low intrinsic activity and intracellular retention.
Significance: THIK2 is a functional but silent channel.

The tandem pore domain halothane-inhibited K^+ channel 1 (THIK1) produces background K^+ currents. Despite 62% amino acid identity with THIK1, THIK2 is not active upon heterologous expression. Here, we show that this apparent lack of activity is due to a unique combination of retention in the endoplasmic reticulum and low intrinsic channel activity at the plasma membrane. A THIK2 mutant containing a proline residue (THIK2-A155P) in its second inner helix (M2) produces K^+-selective currents with properties similar to THIK1, including inhibition by halothane and insensitivity to extracellular pH variations. Another mutation in the M2 helix (I158D) further increases channel activity and affects current kinetics. We also show that the cytoplasmic amino-terminal region of THIK2 (Nt-THIK2) contains an arginine-rich motif (RRSRRR) that acts as a retention/retrieval signal. Mutation of this motif in THIK2 induces a relocation of the channel to the plasma membrane, resulting in measurable currents, even in the absence of mutations in the M2 helix. Cell surface delivery of a Nt-THIK2-CD161 chimera is increased by mutating the arginines of the retention motif but also by converting the serine embedded in this motif to aspartate, suggesting a phosphorylation-dependent regulation of THIK2 trafficking.

Two-pore domain K^+ channels (K_{2P} channels)[3] are present in many cell types, from plants to humans. They produce background K^+ conductances that control the resting membrane potential and influence cell excitability. K_{2P} channels are involved in functions as diverse as cell volume regulation, apoptosis, adrenal gland development and primary hyperaldosteronism, vasodilatation, neuronal excitability and altered motor performance, central O_2 chemoreception and breathing control, perception of pain, polyunsaturated fatty acid-mediated neuroprotection, and mood control (1–3). K_{2P} channels are active as dimers of subunits containing four membrane-spanning helices (M1 to M4) and two pore domains (P1 and P2). They share the same pore architecture with the other families of K^+ channels (4, 5). The upper part of the pore is constricted over a narrow span, termed the selectivity filter, that contains the K^+ channel signature sequence (GYG). This highly conserved region plays key roles in K^+ selectivity and channel gating. The rest of the pore is surrounded by the inner helices (M2 and M4 for K_{2P} channels) that delineate a large vestibule and contribute to the channel gating. Of 15 human genes coding for K_{2P} channels, six subfamilies have been deduced from sequence homology, functional properties, and regulations (1). TWIK1 and TWIK2 form a group of channels with low basal activity and weak inward rectification. TREK1, TREK2, and TRAAK form a group of mechanosensitive channels. TASK1 and TASK3 are inhibited by extracellular acidification, whereas TALK1, TALK2, and TASK2 are activated by extracellular alkalinization. TRESK is the unique member of its own group. Finally, THIK1 (KCNK13, K_{2P}13.1) and THIK2 (KCNK12, K_{2P}12.1) channels form the last subfamily of K_{2P} channels. THIK1 produces background K^+ currents that are inhibited by halothane when expressed in heterologous systems (6). THIK2, as well as TWIK1-related KCNK7 and TASK1-related TASK5, are not active in heterologous expression systems (6–9). These

* The work was supported by Fondation pour la Recherche Médicale Grant Equipe labellisée FRM 2011 and by Agence Nationale de la Recherche Laboratory of Excellence "Ion Channel Science and Therapeutics" Grant ANR-11-LABX-0015-01.
[S] This article contains a supplemental table.
[1] Both authors contributed equally to this work.
[2] To whom correspondence should be addressed: Institut de Pharmacologie Moléculaire et Cellulaire, 660 Route des Lucioles, 06560 Valbonne, France. Tel.: 33-4-93-95-77-27; Fax: 33-4-93-95-77-04; E-mail: lesage@ipmc.cnrs.fr.
[3] The abbreviations used are: K_{2P} channel, two-pore domain K^+ channel; ER, endoplasmic reticulum; THIK, tandem pore domain halothane-inhibited K^+ channel; TWIK, tandem of P domains in a weak inward rectifying K^+ channel; TREK, TWIK-related K^+ channel; TRAAK, TWIK-related arachidonic acid-stimulated K^+ channel; TASK, TWIK-related acid-sensitive K^+ channel; TALK, TWIK-related alkaline pH-activated K^+ channel; TRESK, TWIK-related spinal cord K^+ channel; GIRK, G protein-coupled inwardly rectifying K^+ channel; SUR, sulfonylurea receptor; C-ter, carboxyl-terminal/C terminus; N-ter, amino-terminal/amino terminus; COPI, coat protein I; APC, allophycocyanin; MDCK, Madin-Darby canine kidney; EGFP, enhanced GFP.

"silent" subunits were classified according to their sequence homology with the other members of the K_{2P} family.

Multiple reasons can explain the lack of activity of an ion channel. Channels present at the plasma membrane can require a stimulatory regulator to be active or be maintained silent by an inhibitory factor. Such regulatory mechanisms control gating and activity of K_{ir} channels. For GIRK ($K_{ir}3.x$) channels, the binding of $G\beta\gamma$ is necessary for channel opening (10). On the contrary, K_{ATP} channels ($K_{ir}6.x$) are maintained closed by a high ATP/ADP ratio (11). Channel density in the plasma membrane can also be tightly regulated. Once again, GIRK and K_{ATP} channels are good examples of such a control. The GIRK1 subunit cannot reach the cell surface in the absence of other GIRK subunits (12), and ATP-sensitive $K_{ir}6.2$ subunits are retained in intracellular compartment in the absence of their SUR partner proteins (13). For K_{2P} channels, very few examples of such a control have been reported yet. Surface expression of TASK1 is under the control of regulatory proteins, p11, 14-3-3 and COPI, which compete for their binding to the carboxy-terminal region (C-ter) of the channel (14–17). By combining mutagenesis, electrophysiology, and immunocytochemistry, we have shown that the weak expression of TWIK1 in heterologous expression systems was due to a combination of weak basal activity at the plasma membrane (18) and intracellular retention in recycling endosomes (19, 20). Here we have addressed the functionality of THIK2 by using the same type of approach. By mutating key residues involved in the gating of other K^+ channels or by investigating other molecular determinants deduced from the crystallographic structure of TWIK1 and TRAAK (4, 5), we succeeded in obtaining functional expression of THIK2. Electrophysiological properties and regulations of THIK2 confirm its close relationship with THIK1. Besides its low activity at rest, we also show that THIK2 is mainly present in the endoplasmic reticulum (ER) because of a retention/retrieval motif localized in the amino-terminal part (N-ter) of the channel.

EXPERIMENTAL PROCEDURES

Constructs—Human THIK1 (KCNK13) was cloned into the HindIII/XhoI sites of a derivative of the pGEM vector, pLIN vector for *Xenopus* oocyte expression, or a pcDNA3.1 vector (Invitrogen) for expression in mammalian cells. Human THIK2 (KCNK12) was cloned into the HindIII/BamHI sites of the pLIN and pcDNA3 vectors. Myc (EQKLISEEDL) and HA (YPYDVPDYA) tags were inserted by PCR at the C-ter of THIK1 and THIK2, respectively. Site-directed mutagenesis was carried out by PCR of the full-length plasmid and by using Pfu Turbo DNA polymerase (Agilent Technologies). The entire cDNA was sequenced. N-ter deletion constructs were generated by PCR on the HA-tagged version of THIK2. The mouse TREK1 sequence containing an extracellular HA tag inserted between the second pore domain P2 and the transmembrane segment M4 has been described earlier (21). To construct pEFGP-IRES2-EGFP, a second EGFP sequence was inserted by PCR into the pIRES2-EGFP vector (Clontech). Cloning of the human CD161 into the pIRES2-EGFP vector has been described in Ref. 22. Wild-type and mutated versions of the N-ter of THIK2 were fused by overlapping PCR directly to the N-ter of CD161 and cloned into EcoRI/BamHI sites of pIRES2-EGFP.

Oocyte Expression and Electrophysiology—Capped cRNA was synthesized by using the AmpliCap-Max T7 High Yield Message Maker kit (Cellscript), and THIK plasmids were linearized by AflII. RNA concentration was quantified using a Nanodrop (Thermo Scientific). RNA quality was checked on an RNA nanochip (Agilent Technologies) using an Agilent 2100 bionalyzer. Stage V-VI *Xenopus laevis* oocytes were collected, injected with 1–10 ng of each cRNA, and maintained at 18 °C in ND96 solution (96 mM NaCl, 2 mM KCl, 2 mM $MgCl_2$, 1.8 mM $CaCl_2$, and 5 mM Hepes (pH 7.4)). Oocytes were used 1–3 days after injection. Macroscopic currents were recorded with a two-electrode voltage clamp (Dagan TEV 200 amplifier). Electrodes were filled with 3 M KCl and had a resistance of 0.5–2 MΩ. A small chamber with a perfusion system was used to change extracellular solutions and was connected to the ground by a 3 M KCl-agarose bridge. All constructs were recorded in ND96, and the pH 7.4 was adjusted with NaOH. Stimulation of the preparation, data acquisition, and analysis were performed using pClamp software (Molecular Devices). For ion selectivity measurements, a series of solutions was prepared starting with 0 mM potassium (98 mM NaCl, 0 mM KCl, 1.8 mM $CaCl_2$, 2 mM $MgCl_2$, and 5 mM Hepes) and then by progressive substitution of NaCl by KCl (2, 5, 10, 50, and 98 mM). The pH was adjusted to 7.4 with either NaOH or KOH. For pH sensitivity experiments, all the recordings were done in standard ND96 solution, adjusting the pH with NaOH to values of 6–8. For pH 5.5, the solution was buffered with 5 mM MES, and the pH was adjusted with NaOH. For halothane sensitivity experiments, the recordings were done in standard ND96 solution supplemented with 5 mM halothane as described previously (6). All recordings were done at 20 °C.

Dot Blot—Channel proteins expressed in oocytes were extracted by pipetting up and down in 10 μl/oocyte of a lysis buffer (PBS, 40% (v/v) glycerol, 2% (w/v) CHAPS, 140 mM NaCl, 2 mM EDTA, and 20 mM Tris (pH 8.8), supplemented with a protease inhibitor mixture). After centrifugation at 20,800 × *g* for 30 min at 4 °C, the supernatant was combined with Laemmli loading buffer and dot-blotted in triplicate onto a nitrocellulose membrane. The membranes were blocked in PBS, 0.1% Tween, and 3% BSA and probed with anti-HA (clone 3F10, Roche, 1/1000), anti-Myc (clone 9E10, Roche, 1/1000), or anti-β tubulin (Sigma, 1/200) mouse antibodies and HRP-coupled goat anti-mouse antibody (Jackson ImmunoResearch Laboratories). Chemiluminescent signals were analyzed with FujiFilm fluorescent image analyzer FLA-3000 and quantification was realized using ImageJ software.

MDCK Cell Expression and Immunocytochemistry—Madin-Darby canine kidney (MDCK) cells were grown in 24-well plates onto coverslips and transiently transfected with THIK plasmids using Lipofectamine 2000 (Invitrogen). 24–48 h after transfection, cells were fixed and permeabilized, and channels were labeled with primary anti-HA antibody (clone HA-7, Sigma, 1/1000) or anti-Myc antibody (clone 9E10, Roche, 1/1000), and secondary anti-mouse or anti-rabbit antibodies coupled to Alexa Fluor 488 or Alexa Fluor 594 (Invitrogen). To test for colocalization between THIK channels and the plasma

membrane or ER compartment, an mCherryFP-PH-PLCδ plasmid was cotransfected to visualize the cell surface, or the cells were labeled with anti-calreticulin antibody (catalog no. PA3–900, Thermo Scientific, 1/1000). Coverslips were mounted in Mowiol medium onto slides and observed with a confocal microscope (Leica).

Flow Cytometry—MDCK cells were grown in 35-mm dishes and transiently transfected with CD161 plasmids using Lipofectamine. 48 h after transfection, cells were gently harvested by using PBS and 10 mM EDTA, centrifuged for 5 min at 800 × *g*, and resuspended in PBS, 0.1% BSA, and 0.05% sodium azide incubation solution at 5×10^6 cells/ml. 100 μl of the cells was then incubated for 30 min on ice with APC-conjugated anti-CD161 antibody (Miltenyi Biotec, 1/40) or APC-conjugated mouse IgG2A isotype control antibody (Miltenyi Biotec, 1/40). Cells were washed once with incubation solution and resuspended. Quantification was performed on a BD LSR2 Fortessa using 525/50 band pass (EGFP) and 670/30 band pass (APC) filter sets. Transfected cells were identified as GFP-positive cells. Transfection efficiency was comprised between 41 and 49%. The background level of APC fluorescence was determined by measuring the fluorescence intensity of cells incubated with the mouse IgG2A isotype control. pEGFP-IRES2-EGFP was used as a negative control. Cytometry data were analyzed using the BD CellQuest Pro software (BD Biosciences).

Homology Modeling—The structural model of human THIK2 (UniProt Q9HB15 (430 amino acids), construct [29–321]), was generated on the basis of the structure of human TWIK1 that shares 27% of sequence identity with THIK2. Modeler 9v8 was used to perform the homology modeling of the open form of the dimer complex on the basis of the experimental structure (PDB code 3UKM). The N- and C-ter of THIK2 were removed because no reliable coordinates are available for these regions. The final model was chosen on the basis of its low value of the Modeler objective function, satisfying the Ramachandran plot (MolProbity) and ERRAT and ProQ scores and by visual inspection. No further model optimization was performed.

RESULTS

Introduction of a Proline in the M2 Helix of THIK Channels Enhances K^+ Currents—Despite 62% amino acid identity, THIK1 and THIK2 behave differently upon heterologous expression. THIK1 produces currents, whereas THIK2 gives no measurable current (Fig. 1) (6, 7). Recent crystallographic data on TWIK1 and TRAAK channels suggest that a proline residue in the second membrane-spanning segment (M2) might contribute to helix flexibility and channel opening (4, 5). This proline, which is conserved in most K_{2P} channels, is replaced with a serine in THIK1 (Ser-136) and an alanine in THIK2 (Ala-155) (Fig. 1, *A* and *E*). We tested the possibility that the absence of proline in the M2 domain of THIK2 may be associated with its apparent lack of activity. Replacing Ala-155 with a proline in THIK2 allowed us to record a current (Fig. 1*B*). A significant amount of cRNA (10 ng/oocyte) and 2–3 days of expression were necessary to obtain a THIK2-A155P current of 0.92 ± 0.1 μA, $n = 6$ at 0 mV, compared with 0.11 ± 0.03 μA, $n = 7$ for THIK2 (Fig. 1*C*). The latter value is not significantly different from non-injected oocytes (Fig. 2). Ten times less cRNA and a single day of expression were sufficient to obtain a 1.4 ± 0.13 μA, $n = 11$ current from THIK1-expressing oocytes. Introducing a proline residue in the M2 helix of THIK1 gives a THIK1-S136P channel that is more active than its wild-type counterpart (3.3 ± 0.3 μA, $n = 11$ *versus* 1.4 ± 0.13 μA, $n = 11$). Another parameter consistent with the appearance of a K^+ current in oocytes expressing THIK2-A155P is the reversal potential measured at 0 current (E_{rev}) (Fig. 1*C*). Although E_{rev} is not significantly different between THIK1 (−86 ± 1.2 mV) and THIK1-S136P (−88 ± 1.9 mV) currents, E_{rev} shifts from −45 ± 3 mV for the THIK2 current to −82 ± 2.8 mV for THIK2-A155P. This indicates that THIK2-A155P, like THIK1, is able to drive the membrane potential to values close to the K^+ equilibrium potential (E_K). Interestingly, the current kinetic is different between THIK1 and THIK2-A155P channels (Fig. 1*B*). Activation in response to depolarizing voltage steps is almost instantaneous for THIK1, whereas THIK2-A155P exhibits a slower activation. This property seems to be independent of the inserted proline because THIK1-S136P does not exhibit these particular kinetics. The current increase because of the proline insertion in THIK1 and THIK2 is not due to an increase in total protein synthesis (Fig. 1*D*) or to a better addressing of the channel at the plasma membrane (Fig. 5). TREK1 contains a proline residue in the M2 helix (proline 183, Fig. 1*A*). We replaced this proline by an alanine as in THIK2. As expected, TREK1-P183A produces three times less current than TREK1 (1.54 ± 0.2 μA, $n = 9$ at 0 mV *versus* 0.55 ± 0.14 μA, $n = 11$). Together, these results show that a proline residue in the M2 helix is important for the channel activity of K_{2P} subunits.

Other Mutations in the M2 Inner Helix Stimulate THIK Channel Activity—Besides proline, M2 contains other residues involved in the gating of K_{2P} channels. Three glycines are present in the highly active K_{2P} channels KCNK0 and TREK1 that are replaced by larger hydrophobic residues in TWIK1 (Fig. 1*A*). We have shown that the replacement of these residues by glycines induced a 3-fold increase of current amplitude of TWIK1 (18). The replacement of the first of these hydrophobic residues by an aspartate (L146D) produced a 16-fold increase of the current amplitude (18). In THIK2, residues at these positions are large hydrophobic residues (Ile-158, Leu-163, and Leu-165). Replacing them with glycines was not sufficient to produce measurable currents. However, replacing isoleucine 158 with an aspartate (THIK2-I158D) allowed us to record a current of 0.96 ± 0.01 μA, $n = 11$ at 0 mV (Fig. 2*A*). With THIK2-A155P and THIK2-I158D, we were now able to detect THIK2 currents produced by two different mutant channels. The current increase is comparable between the two mutants, giving a 7-fold increase for THIK2-A155P and a 6-fold increase for THIK2-I158D when compared with currents recorded from non-injected or THIK2-expressing oocytes. Combining both mutations in THIK2-A155P-I158D results in a 19-fold increase of the current amplitude (3.07 ± 0.04 μA at 0 mV, $n = 18$). In addition to its stimulating effect, I158D mutation dramatically affects current kinetics (Fig. 2, *B* and *C*). Currents generated by THIK2-I158D and THIK2-A155P-I158D are not typical for K_{2P} channels. In ND96 solution, the current amplitude at the steady state increases with voltage depolarization until reaching a plateau around 0 mV, from where current amplitude ceases to

increase. This property gives to these channels an I-V relationship that is not linear but saturates upon strong depolarization. E_{rev} for these mutants (−79 mV ± 4, n = 10 for THIK2-I158D and −93 mV ± 1, n = 11 for THIK2-A155P-I158D) are negative as E_{rev} for THIK2-A155P (−81 mV ± 2, n = 11), suggesting that K^+ selectivity is not affected by introducing an aspartate residue in the M2 helix. THIK1 mutant channels containing an aspartate mutation at the equivalent position in M2 (THIK1-

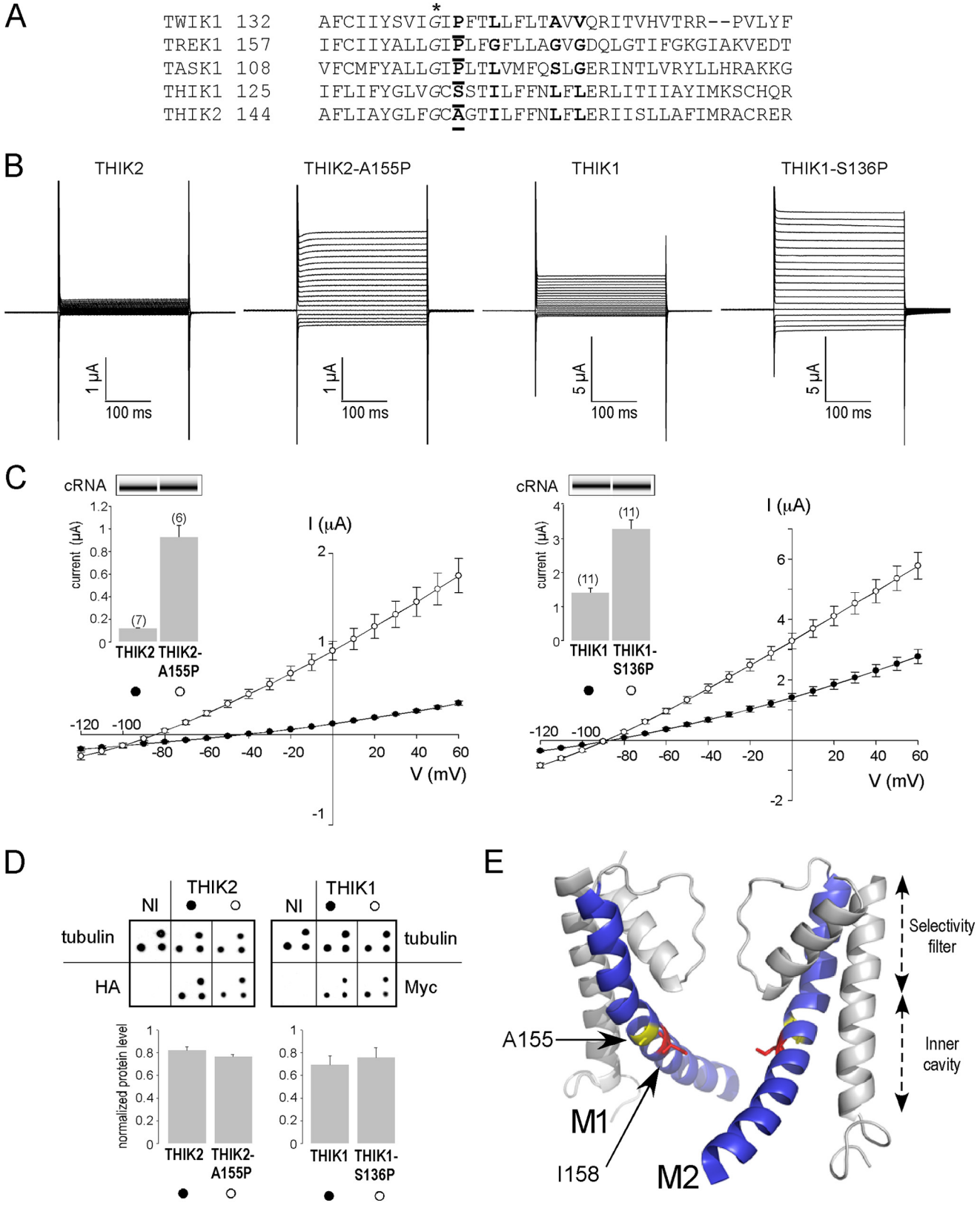

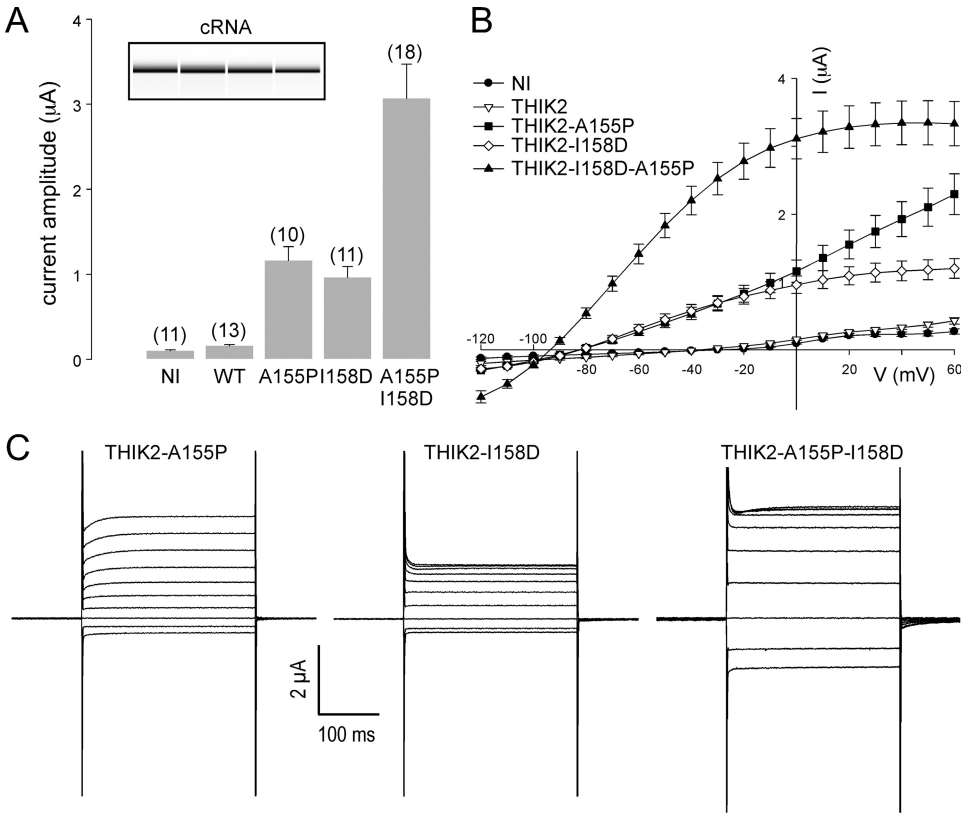

FIGURE 2. **Effect of mutations in the M2 inner helix of THIK2.** *A*, steady-state current amplitude at 0 mV measured from non-injected (*NI*) and THIK2 channel-expressing oocytes (mean ± S.E., $n = 10$ to 18 oocytes/condition as indicated). *Inset*, electrophoresis gel profile of injected cRNAs. *B*, current-voltage relationships. Mean currents were measured at the steady state of the depolarization pulses. *C*, currents elicited by voltage pulses from −120 to +60 mV in 10-mV increments from a holding potential of −80 mV.

I139D) also produce currents that saturate upon strong depolarization (Fig. 3*C*). THIK1-I139D and THIK1-S136P-I139D I-V curves display a rectification that is not observed for THIK1 (Fig. 3*B*). S136P and I139D mutations in THIK1 have a significant effect on the current amplitude but have no additive effects. This difference with THIK2 may be related to the already high channel activity of THIK1 in basal conditions.

Ion Selectivity and Regulation of Proline-containing THIK Channels—We next characterized ion channel selectivity of THIK2-A155P and its regulation by external acidification and halothane. We evaluated the potential effect of the proline mutation on these regulations by comparing THIK1 and THIK1-S136P in the same conditions. The currents were recorded in different concentrations of external K^+ (Fig. 4*A*). The value of E_{rev} was plotted against the K^+ concentration, giving linear regression fits comparable between the different channels. A 10-fold change in external K^+ concentration leads to a -51 ± 3 mV, $n = 5$ shift for THIK2-A155P, consistent with highly selective K^+ channels and not significantly different from -56 ± 2 mV, $n = 6$ for THIK1-S136P or -49 ± 5 mV, $n = 5$ for THIK1. In contrast to most of the other K_{2P} channels (2, 18, 23, 24), THIK1 is insensitive to extracellular pH changes (6). We found that proline-containing THIK1 and THIK2 channels are not affected by changing the external pH of the ND96 solution from pH 8 to 5.5 by 0.5-unit steps (Fig. 4*B*). The most salient property of THIK1 is its inhibition by the volatile anesthetic halothane. THIK2-A155P is also inhibited by halothane, at all depolarization steps, in a range similar to THIK1 and THIK1-S136P (Fig. 4*C*). For comparison, application of 5 mM halothane reduced the current amplitude by 60 ± 7%, $n = 6$ at +30 mV for THIK1-S136P and 58 ± 2%, $n = 6$ for THIK2-A155P, a degree of inhibition comparable with what we and others have reported for human (Fig. 4*C*, *inset*) and rat (6) THIK1 in oocytes (43 ± 3% and 56 ± 5%, respectively).

The Cytoplasmic N-ter of THIK2 Controls Its Cell Trafficking—THIK2 activity is limited by its unique M2 sequence. We also tested the possibility that low current expression may also be due to a restricted amount of channels present in the plasma

FIGURE 1. **Introducing a proline residue in the M2 inner helix of the silent THIK2 subunit produces active channels.** *A*, sequence alignment of human K_{2P} channels. The conserved glycine residue proposed as a hinge is shown in *italics* and indicated with an *asterisk*. The proline residue conserved among all K_{2P} channels, except THIK1 and THIK2, is *underlined* and shown in *boldface*. Glycine residues in TREK1 and the corresponding larger hydrophobic residues in TWIK1, THIK1, and THIK2 are also shown in *boldface*. *B*, currents elicited by voltage pulses from −120 to +60 mV in 10-mV increments from a holding potential of −80 mV. *C*, current-voltage relationships. Mean currents were measured at the end of voltage pulses (steady-state). *Insets*, mean steady-state currents at 0 mV. Electrophoresis gel profiles of injected cRNAs are shown. *D*, after recording, oocytes in *C* were solubilized, and lysates were spotted on membrane in triplicate. HA-tagged THIK2 and Myc-tagged THIK1 channels were detected using anti-HA and anti-Myc antibodies. Total protein expression was normalized to the endogenous tubulin content using anti-tubulin antibody and quantified using ImageJ software. *NI*, non-injected oocytes. *E*, structural modeling of a THIK2 dimer. Shown is a side view of the selectivity filter and of the transmembrane segments M1 and M2 surrounding the inner cavity. The cytoplasmic N- and C-ter domains, transmembrane segments M3 and M4, and the extracellular domains of THIK2 are not depicted.

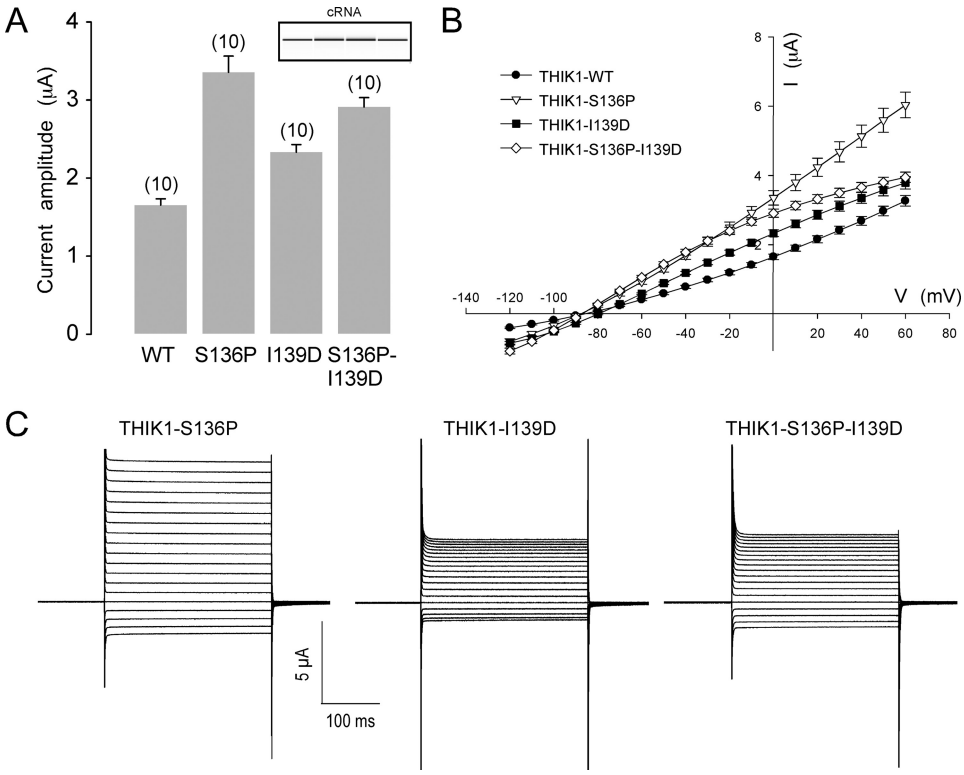

FIGURE 3. **Effect of mutations in the M2 inner helix of THIK1.** *A*, steady-state currents measured at 0 mV from *Xenopus* oocytes expressing THIK1, THIK1-S136P, THIK1-I139D, and THIK1-S136P-I139D (mean ± S.E., $n = 10$). *Inset*, electrophoresis gel profile of injected cRNAs. *B*, current-voltage relationships. Currents are measured at the end of the depolarization pulse (mean ± S.E., $n = 10$). *C*, currents elicited by voltage pulses from −120 to +60 mV in 10-mV increments from a holding potential of −80 mV.

membrane. We expressed THIK channels in MDCK cells and followed their distribution by immunofluorescence. Although THIK1 is largely present at the cell surface of transfected MDCK cells, THIK2 is mainly distributed in intracellular compartments in a fine reticular network extending through the cytoplasm (Fig. 5). Colocalization with plasma membrane (mCherryFP-PH-PLCδ) or ER (calreticulin) markers demonstrates that THIK1 channels are mostly localized in the plasma membrane, whereas THIK2 channels are predominantly retained in the ER (Fig. 5). Trafficking motifs being often located in the cytoplasmic regions of membrane proteins, we compared the N-ter of THIK1 and THIK2 (Fig. 6*A*). Because this alignment did not show any sequence homology, we progressively deleted the N-ter of THIK2, 10 amino acids at a time, and followed cell distribution of these mutants (Fig. 6*B*). The THIK2-Δ10 channel has the same ER distribution as THIK2, whereas a large part of THIK2-Δ20 and THIK2-Δ30 channels is relocated at the cell surface (Fig. 6*B*). These results suggest that an ER retention/retrieval signal is present in the cytoplasmic N-ter of THIK2 between residues 11 and 20. Arginine-based ER retention/retrieval signals have been identified in membrane proteins (13, 25–27). THIK2 N-ter contains 10 arginine residues and, among them, five are clustered between residues 11 and 16 in a motif (RRSRRR) that resembles the R*X*R motif responsible for the ER retention of K_{ATP} channel subunits ($K_{ir}6.2$ and SUR1), glutamate receptor subunits GluN1 and KA2, and the $GABA_B$ R1 subunit (13, 25–27). We mutated arginines that might constitute two possible motifs in THIK2 (RSRR or RRR according to the database of eukaryotic linear motifs, ELM). As expected, the mutant THIK2-R11A-R12A-R14A-R15A-R16A (named THIK2–5RA), redistributes to the plasma membrane (Fig. 6*B*). This effect shows that an arginine-based motif is involved in the control of THIK2 trafficking. Moreover, adding the N-ter of THIK2 to TREK1 completely abolishes its localization at the plasma membrane (Fig. 6*C*). This demonstrates that this region of THIK2 contains a retention signal that is dominant over possible forward signals. Finally, we tested the effect of the deletion of the N-ter alone and in combination with M2 mutations (Fig. 6*D*). THIK2-Δ30 generates currents of 0.42 ± 0.03 μA, $n = 8$ compared with 0.08 ± 0.01 μA, $n = 8$ in oocytes expressing THIK2 (Fig. 6*D*, *left panel*). THIK2-Δ30 currents are limited but 5-fold higher than THIK2, a result in good agreement with the relocation of THIK2-Δ30 to the plasma membrane in transfected cells. We then compared the amplitude of THIK2-A155P and THIK2-A155P-I158D currents with THIK2-Δ30-A155P and THIK2-Δ30-A155P-I158D currents (supplemental table). Once again, the deletion of the N-ter induces a current increase that is additive to the effect of the M2 mutations. THIK2-Δ30-A155P-I158D produces 143 times more current than THIK2, 11.5 ± 1.4 μA, $n = 6$ *versus* 0.08 ± 0.01 μA, $n = 8$ at 0 mV (Fig. 6*D*, *right panel*). The same types of results were obtained by mutating the arginine residues to promote THIK2 expression in the plasma membrane (supplemental table). THIK2–5RA-A155P-I158D gives 12 times more current than THIK2-A155P-I158D (8.7 ± 1.3 μA, $n = 4$ at 0 mV *versus* 0.7 ± 0.1 μA, $n = 4$) and 174 times more than THIK2 (0.05 ± 0.007 μA, $n = 4$).

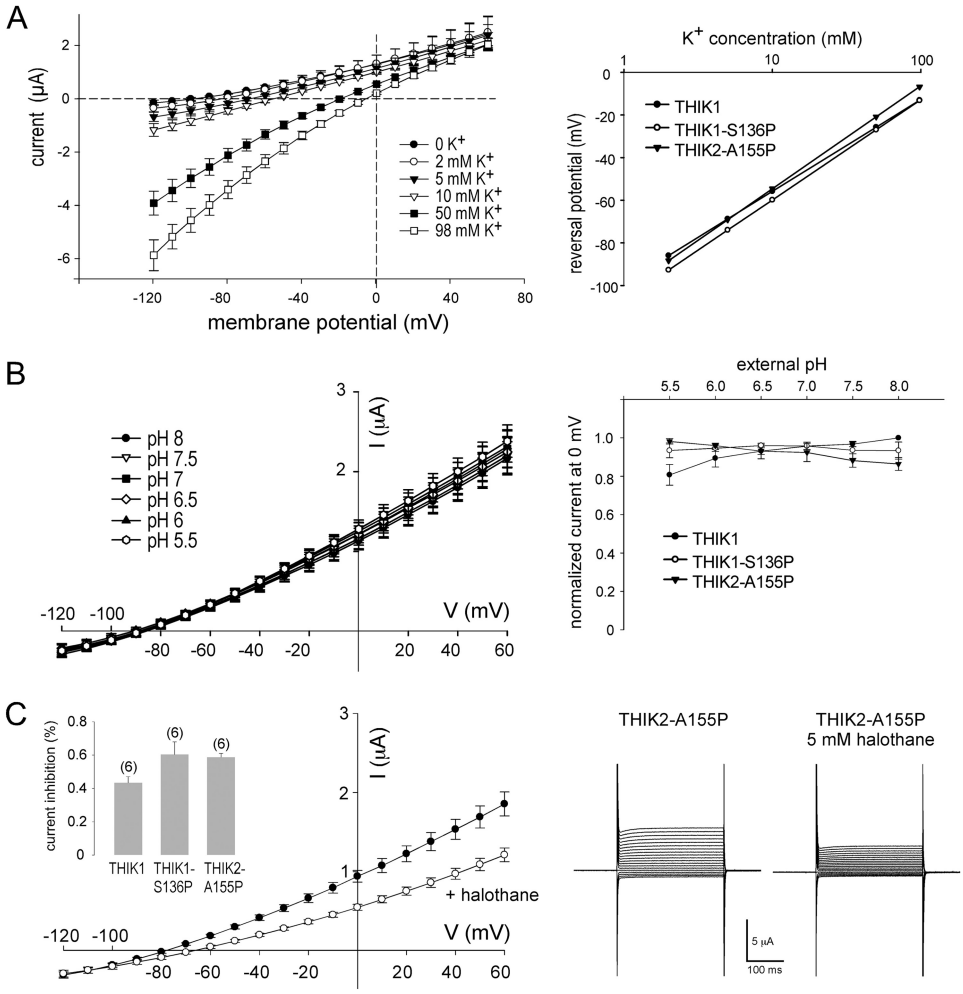

FIGURE 4. **THIK1 and THIK2 share similar electrophysiological properties and regulations.** *A*, *left panel*, current-voltage relationships. Mean currents were recorded at the steady state from oocytes expressing THIK2-A155P. *Right panel*, reversal potential as a function of external K^+ concentration (mean ± S.E., n = 5–6). *B*, *left panel*, current-voltage relationships. Mean current were recorded at the steady state from oocytes expressing THIK2-A155P bathed in ND96 with different pH values from 8–5.5 by 0.5-unit decrements (mean ± S.E., n = 6). *Right panel*, normalized currents measured at 0 mV and plotted against the extracellular pH values. *C*, *left panel*, current-voltage relationships measured from oocytes expressing THIK2-A155P successively bathed in ND96 (●) and ND96 + 5 mM halothane (○). *Inset*, percentage of current inhibition at +30 mV by 5 mM halothane. *Right panel*, currents elicited by voltage pulses from −120 to +60 mV in 10-mV increments from a holding potential of −80 mV.

The ER Retention/Retrieval Signal in THIK2 May Be Regulated by Phosphorylation—To identify relevant residues in the ER retention motif, we grafted the first 30 amino acids of THIK2 to the N-ter of human CD161, a type II transmembrane protein unrelated to ion channels (22). This approach has been used extensively to study forward and endocytic trafficking signals in various channels and receptors (13, 28–30). To quantify the surface expression of CD161 and chimeric Nt-THIK2-CD161, we performed flow cytometry on transfected MDCK cells labeled with anti-CD161 antibody conjugated to the fluorescent dye APC. All sequences were cloned into pIRES2-EGFP to quantify CD161 fluorescence only from transfected GFP-positive cells. Cells expressing pEGFP-IRES2-EGFP were used as a negative control for anti-CD161 antibodies (Fig. 7*A*), and cells labeled with APC-conjugated mouse IgG2A isotype control antibody were used to evaluate the background signal (Fig. 7, *filled histograms*). As reported in other cell lines, CD161 displayed strong surface expression in MDCK cells (22). The dot plot of fluorescence for CD161-transfected cells illustrates the coexpression of GFP and CD161 in the *upper right quadrant* (Fig. 7*A*), giving a fluorescence intensity median value of 382 for CD161 labeling (*B*, *red line*). We then compared the histograms and median values of CD161-transfected cells with cells expressing the Nt-THIK2-CD161 chimera. A strong shift was observed toward lower surface fluorescence intensity, the median value shifting from 382 (*red line*) to 81 (*blue line*) (Fig. 7*C*). This indicates that the fusion of the THIK2 N-ter to CD161 restricts Nt-THIK2-CD161 trafficking to the plasma membrane. Mutating arginines of the ER retention/retrieval motif (Nt-5RA-THIK2-CD161) almost restored normal surface trafficking (median value of 269, Fig. 7*C*, *blue line*). In the different experiments, transfection efficiency was similar. These results demonstrate that the N-ter of THIK2 is sufficient to limit surface expression of membrane proteins. Embedded in the five-arginine sequence of the ER retention motif is a serine residue ($RRS_{13}RRR$) that forms a consensus site (R*X*S/T) for phosphorylation by PKA. In the PHOSIDA posttranslational modification database, serine 13 displays a high accessibility for phosphorylation. On the other hand, in HeLa cells, the peptide corresponding to the surrounding

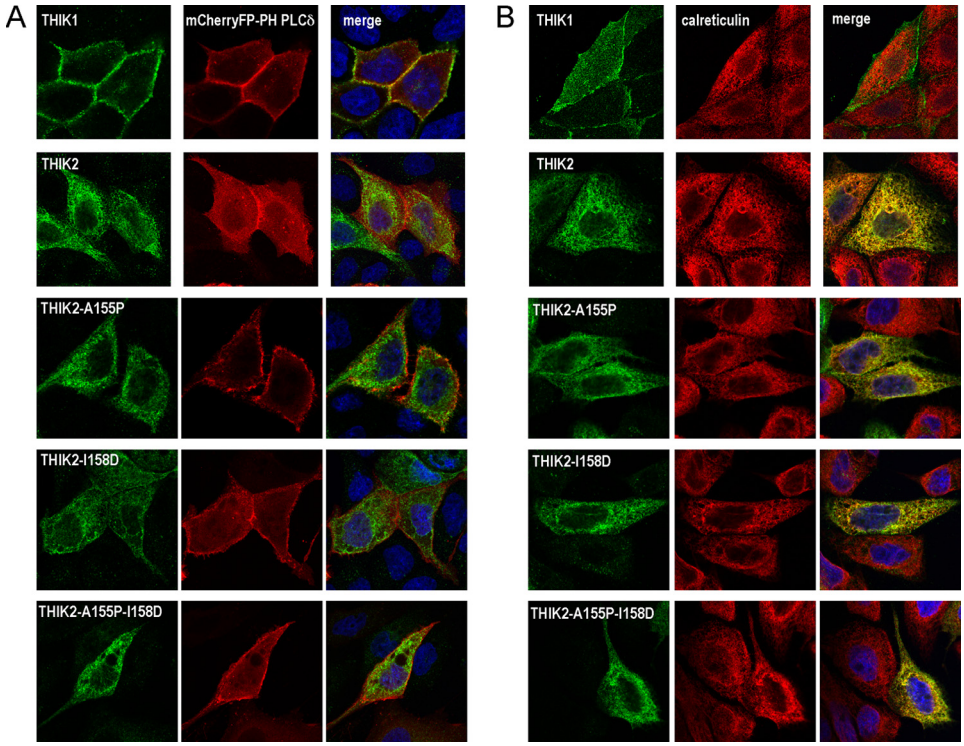

FIGURE 5. **Colocalization of THIK channels with markers of the plasma membrane and endoplasmic reticulum.** *A*, MDCK cells were cotransfected with plasmids for expression of a plasma membrane marker, mCherryFP-PH-PLCδ (*red*), and THIK1-Myc- or HA-tagged THIK2 and THIK2 mutant constructs. 24–48 h after transfection, cells were fixed, permeabilized, and labeled with primary anti-Myc antibody or anti-HA antibody and secondary antibodies coupled to Alexa Fluor 488 (*green*). *B*, cells expressing THIK1-Myc or HA-tagged THIK2 and THIK2 mutants were labeled with primary anti-Myc antibody or anti-HA antibody and anti-calreticulin and secondary antibodies coupled to Alexa Fluor 488 (channels in *green*) or to Alexa Fluor 594 (calreticulin, *red*).

sequence (PRPPPRRS$_{13}$RRRLPRP) is phosphorylated, suggesting that THIK2 is phosphorylated at position 13 (31, 32). We mutated this serine to alanine (S13A in Nt-S13A-THIK2-CD161) to prevent any potential phosphorylation or to aspartate (S13D in Nt-S13D-THIK2-CD161) to mimic phosphorylation. Flow cytometry quantification of CD161 surface expression showed that Nt-S13A-THIK2-CD161 was detected at a lower level in the plasma membrane compared with CD161, as shown by a shift in the median value from 382 to 49, a value even lower than that of Nt-THIK2-CD161 (81; Fig. 7, *C* and *D*). This suggests that basal phosphorylation of serine 13 in THIK2 could be responsible for the modest but measurable current expression of THIK2-A155P and THIK2-A155P-I158D in the absence of any mutations in the retention signal (Fig. 6*D*). Nt-S13D-THIK2-CD161 protein is detected at higher levels at the plasma membrane (median value of 173) than Nt-S13A-THIK2-CD161 and Nt-THIK2-CD161 (Fig. 7*D*), demonstrating that mimicking phosphorylation of serine 13 by introducing a negatively charged residue promotes cell surface delivery. This effect is not as strong as mutating surrounding arginines but suggests that trafficking of THIK2 from the ER to the plasma membrane is regulated in a phosphorylation-dependent manner (Fig. 7*E*). Finally, we tested the effect of mutating serine 13 on THIK2 current density in oocytes. The S13A and S13D mutations were introduced into the active THIK2-A155P channel, and currents were recorded 2 days after injection of 10 ng of cRNA. Interestingly, no significant difference in current density was observed between THIK2-A155P and THIK2-S13A-A155P, whereas a 30% increased was obtained with THIK2-S13D-A155P (Fig. 7*F* and supplemental table). This current increase associated with the S13D mutation suggests that phosphorylation of serine 13 affects the retrieval/retention signal and helps THIK2 to exit the ER and to reach the plasma membrane.

DISCUSSION

Xenopus oocytes are widely used for studying ion channels in a controlled *in vivo* environment. Oocytes do not express a lot of endogenous ion channels, and currents from injected RNAs are usually much larger than endogenous currents. In addition, the oocyte system is particularly well suited for the characterization of mutations because injection and electrophysiology can be carried out rapidly and in a semi-automated fashion. Another advantage is to get an excellent control of the expression level by combining time of expression and quantity of injected cRNAs. Here, it was particularly important to compare the very different expression levels of THIK1, THIK2 and mutant THIK channels. However, because of its large size and autofluorescence in the green, oocytes cannot be used for trafficking studies by imaging methods. For this reason, we used MDCK cells, which have proven to be a good model for cell biology, particularly to study the trafficking of membrane receptors and ion channels. However, these cells are not really good for electrophysiological characterization of recombinant channels because they express endogenous currents, including K^+ currents. Also, it would have been very difficult to control the expression levels in these cells by using transfected plasmids. We combined electrophysiology in oocytes and traffick-

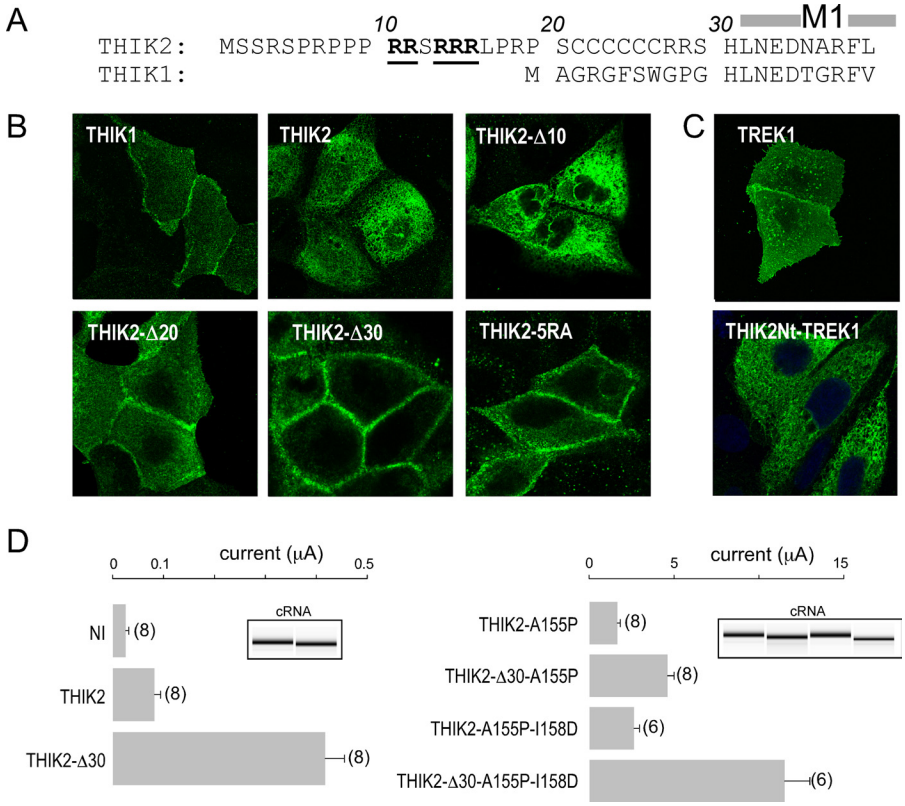

FIGURE 6. **The cytoplasmic N-ter of THIK2 contains an ER retention/retrieval signal.** *A*, alignment of the THIK2 and THIK1 N-ter domains. M1 is the first membrane-spanning helix. Arginine residues in the retention motif are shown in *boldface*. *B*, confocal images of transfected MDCK cells. Expressed channels are labeled in *green*. *C*, confocal images of MDCK cells expressing HA-tagged TREK1 or HA-tagged TREK1 containing the N-ter of THIK2 (*THIK2Nt-TREK1*). Expressed channels are labeled in *green*. *D*, mean currents measured at 0 mV from non-injected oocytes (*NI*) and from oocytes expressing wild-type or mutated THIK2 channels (mean ± S.E., $n = 6–8$). *Insets*, electrophoresis gel profiles of injected cRNAs.

ing studies in MDCK cells to keep only the advantages of both expression systems. Trafficking in oocytes and MDCK cells is certainly not identical but very similar, the vertebrate *Xenopus* oocyte using the same overall cell machinery than mammalian cells. There are many examples of studies showing that the trafficking of membrane proteins are regulated in a same way in oocytes and mammalian cells, in particular for control of ER retention by basic motifs, for example with ATP-sensitive K^+ channels (13) and $GABA_B$ receptors (25). By combining oocytes and MDCK cells, we have demonstrated previously that TWIK1 activity was regulated by a combination of intracellular recycling and low activity at the plasma membrane (18, 20). Together, our results indicate that THIK2 is a functional channel and that its apparent lack of function is due to low channel activity and intracellular retention.

Molecular Determinants of THIK Channel Gating—For K_v channels, a proline-based motif (P*X*P), located in the S6 inner helix, is essential for channel opening upon depolarization (33, 34). For K_{ir} channels, a conserved glycine in the M2 inner helix has been proposed as a hinge, allowing the spreading of the inner helices and the opening of the lower part of the pore (35, 36). Proline and glycine residues in the M2 and M4 inner helices are also conserved in K_{2P} channels and might contribute to channel opening. In the x-ray structure of TWIK1, the M2 inner helix is kinked by ~20° at proline 143 (5). The same holds true in TRAAK, in which the two M2 helices project laterally after the kink at proline 155, leaving the vestibule open to the cytoplasmic solution (4). Here we found that introducing a proline residue at an equivalent position in THIK channels increases THIK activity. However, the presence of this proline is not a prerequisite to channel opening because THIK1 (Fig. 1*B*) and THIK2-Δ30 (Fig. 6*D*) also generate currents, despite the absence of a proline in M2. The importance of glycine residues in M2 varies between K_{2P} channels. KCNK0 and TREK/TRAAK channels have three glycines, whereas TASK and TALK channels have only one glycine conserved (the third one, Fig. 1*A*). THIK and TWIK channels have no glycine but larger hydrophobic residues. Introducing glycines in TWIK1 stimulates channel activity (18), but this has no effect on THIK channels. However, introducing a negative charge in TWIK1, THIK1, and THIK2 at the equivalent position of the first glycine in KCNK0 increases current amplitude. The mechanism of activation in TWIK and THIK channels is not known, but introducing an aspartate at a homologous position in KCNK0 and $K_{ir}3.2$ channels increases open channel probability (37, 38). Alternatively, this residue is facing the conduction pathway, and the presence of rings of negative charges along the permeation pathway of other K^+ channels has been shown to dramatically affect K^+ channel conductance (39). This effect is due to an electrostatic mechanism, the negative charges altering the electrical potential, thus increasing local K^+ concentration.

THIK Channel Trafficking—Trafficking of membrane proteins is influenced by ER retention/retrieval, ER export, and/or endocytosis signals. This has been shown for TASK1 and

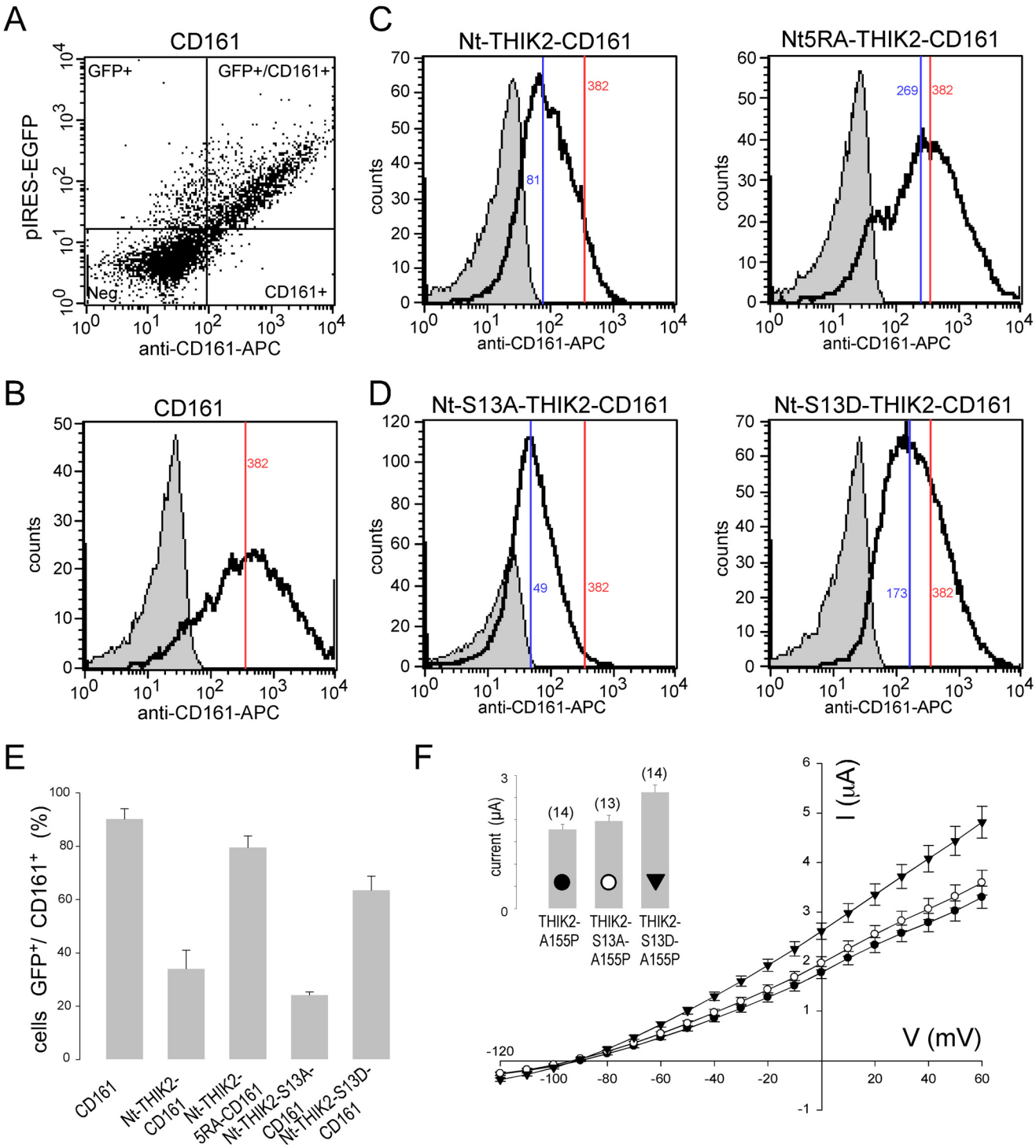

FIGURE 7. **Mutation of serine 13 in THIK2 N-ter affects surface expression of the Nt-THIK2-CD161 chimera.** MDCK cells expressing CD161 and various Nt-THIK2-CD161 chimeras were labeled with anti-CD161 antibody and analyzed by flow cytometry. *A*, viable and singulet cells transfected with pCD161-IRES2-EGFP were separated into four distinct populations according to their level of total protein expression (GFP) and surface protein expression (CD161). *B*, *C*, and *D*, CD161 expression was analyzed on gated GFP-positive cells using anti-CD161-APC (*empty histogram*) against isotype control APC (*filled histogram*) on CD161- (*B*), Nt-THIK2-CD161- or Nt5RA-THIK2-CD161- (*C*), and Nt-S13A-THIK2-CD161- or Nt-S13D-THIK2-CD161-transfected (*D*) MDCK cells. The *red vertical line* indicates the median value of CD161 fluorescence and serves as reference to compare with the median value of each chimera (*blue vertical line*). *E*, histogram combining data from four independent experiments. *F*, expression of THIK2-A155P, THIK2-S13A-155P, and THIK2-S13D-A155P channels in *Xenopus* oocytes.

TWIK1 K_{2P} channels (for a review, see Ref. 40). TWIK1 contains a di-isoleucine motif in its cytoplasmic C-ter that restricts its localization at the cell surface and redistributes the channel to the recycling endosomes by a rapid and constitutive endocytosis (20). Mutation of this motif stabilizes the channel at the cell surface, resulting in a 3-fold increase of the current recorded in oocytes. Here, we found that THIK2 contains an ER trafficking signal in its cytoplasmic N-ter that limits its expression in the plasma membrane by maintaining the channel in the ER. Progressive deletions and mutations narrowed the signal to

a six- amino acid motif (RRSRRR) that resembles arginine-based ER retention motifs described in several ion channels and receptors (13, 25–27). Those motifs retain newly synthesized proteins in the ER, probably by binding to resident chaperone proteins. Stable assembling or reversible binding to other proteins that mask the retention signal can relieve this block, allowing exit from the ER and trafficking to the plasma membrane. ER retention can also be the consequence of a retrieval of the protein from the Golgi to the ER, notably *via* a COPI-dependent vesicular transport. Because it is difficult to distinguish between the two mechanisms, those signals are named ER retention/retrieval motifs (for a review, see Ref. 41). Looking for THIK2 protein partners may provide a better understanding of the mechanisms used by cells to regulate surface expression of THIK2. Phosphorylation-dependent surface targeting can also enable the regulation of surface expression of channels and receptors (for a review, see Ref. 41). ER retention of an alternatively spliced isoform of the GluN1 subunit of *N*-methyl-D-aspartate receptors is regulated by PKA and PKC phosphorylations (29, 42). Also, PKA-dependent phosphorylation of a serine in the N-ter of ROMK1 ($K_{ir}1.1$) suppresses an ER retention signal located in the C-ter, increasing channel delivery to the cell surface (43). For TASK1 channels, binding of 14-3-3, which promotes channel forward trafficking to the plasma membrane, depends on the phosphorylation by PKA of a serine located in a dibasic motif situated in the cytoplasmic C-ter of the channel (44). The arginine-based motif in the N-ter of THIK2 contains a serine residue that is a potential site of phosphorylation by PKA. Preventing phosphorylation reduces surface expression of a chimera containing the N-ter of THIK2, whereas mimicking constitutive phosphorylation promotes trafficking to the cell surface (Fig. 7*E*). Moreover, introducing a mutation mimicking phosphorylation in THIK2 (S13D) leads to an increase of the current density in oocytes (Fig. 7*F*). The effect of the mutation is less important than in the CD161 fusion protein containing only the N-ter of THIK2, suggesting that other sites may be involved in the trafficking of THIK2. Such a regulatory mechanism, by altering the efficiency of THIK2 channel surface expression, may influence cellular excitability on a more dynamic basis by providing the cells with a pool of releasable channels.

Perspectives—THIK1 and THIK2 have different patterns of expression in the kidney and the brain (6, 45). In the cerebellum and several specific nuclei (amygdala basolateral nuclei, thalamus ventral posterior nuclei, oculomotor nucleus, and so forth) where THIK1 is not detected, THIK2 is highly expressed (6). Native background K^+ conductance with characteristic similar to THIK channels (including inhibition by halothane and insensitivity to pH) has already been identified in a specific neuronal population, such as respiratory neurons, Purkinje cells, and rat trigeminal ganglion neurons (46–49). By demonstrating that THIK2 is a functional channel, this work suggests that THIK2 plays a role in these neurons, acting alone or in combination with THIK1 to regulate resting membrane potential and cell excitability. THIK2 might require either an accessory subunit or specific intracellular regulations, notably via phosphorylation, to reach the plasma membrane. Using THIK2-A155P-I158D, which produces more current than THIK2 in the plasma membrane, should help to study the regulation of THIK2 forward trafficking by following current variations at the plasma membrane. The weak activity of THIK2 in the plasma membrane also suggests that, in native systems, other regulatory mechanisms are necessary to directly stimulate THIK2 activity when the channel reaches the plasma membrane. Expression of a THIK2 mutant that is less retained in the ER, such as THIK2–5RA, should help to test such signaling pathways by dissociating current increases related to channel stimulation from current increases related to channel trafficking.

Acknowledgments—We thank Nathalie Leroudier for technical assistance with sequencing analysis, Julie Cazareth for flow cytometry measurements, the members of the genomic platform for RNA analysis (Agilent), and Frederic Brau for confocal microscopy. We also thank Arnaud Echard and Franck Perez for the mCherryFP-PH PLCδ plasmid, Amanda Patel for pEGFP-IRES2-EGFP, Thomas Besson for technical assistance, and Michael Grabe for comments.

REFERENCES

1. Enyedi, P., and Czirják, G. (2010) Molecular background of leak K^+ currents. Two-pore domain potassium channels. *Physiol. Rev.* **90,** 559–605
2. Lesage, F., and Barhanin, J. (2011) Molecular physiology of pH-sensitive K2P channels. *Physiology* **26,** 424–437
3. Noël, J., Sandoz, G., and Lesage, F. (2011) Molecular regulations governing TREK and TRAAK channel functions. *Channels* **5,** 402–409
4. Brohawn, S. G., del Mármol, J., and MacKinnon, R. (2012) Crystal structure of the human K2P TRAAK, a lipid- and mechano-sensitive K^+ ion channel. *Science* **335,** 436–441
5. Miller, A. N., and Long, S. B. (2012) Crystal structure of the human two-pore domain potassium channel K2P1. *Science* **335,** 432–436
6. Rajan, S., Wischmeyer, E., Karschin, C., Preisig-Müller, R., Grzeschik, K. H., Daut, J., Karschin, A., and Derst, C. (2001) THIK-1 and THIK-2, a novel subfamily of tandem pore domain K^+ channels. *J. Biol. Chem.* **276,** 7302–7311
7. Girard, C., Duprat, F., Terrenoire, C., Tinel, N., Fosset, M., Romey, G., Lazdunski, M., and Lesage, F. (2001) Genomic and functional characteristics of novel human pancreatic 2P domain K^+ channels. *Biochem. Biophys. Res. Commun.* **282,** 249–256
8. Kim, D., and Gnatenco, C. (2001) TASK-5, a new member of the tandem-pore K^+ channel family. *Biochem. Biophys. Res. Commun.* **284,** 923–930
9. Salinas, M., Reyes, R., Lesage, F., Fosset, M., Heurteaux, C., Romey, G., and Lazdunski, M. (1999) Cloning of a new mouse two-P domain channel subunit and a human homologue with a unique pore structure. *J. Biol. Chem.* **274,** 11751–11760
10. Logothetis, D. E., Kurachi, Y., Galper, J., Neer, E. J., and Clapham, D. E. (1987) The $\beta\gamma$ subunits of GTP-binding proteins activate the muscarinic K^+ channel in heart. *Nature* **325,** 321–326
11. Noma, A. (1983) ATP-regulated K^+ channels in cardiac muscle. *Nature* **305,** 147–148
12. Ma, D., Zerangue, N., Raab-Graham, K., Fried, S. R., Jan, Y. N., and Jan, L. Y. (2002) Diverse trafficking patterns due to multiple traffic motifs in G protein-activated inwardly rectifying potassium channels from brain and heart. *Neuron* **33,** 715–729
13. Zerangue, N., Schwappach, B., Jan, Y. N., and Jan, L. Y. (1999) A new ER trafficking signal regulates the subunit stoichiometry of plasma membrane K(ATP) channels. *Neuron* **22,** 537–548
14. Girard, C., Tinel, N., Terrenoire, C., Romey, G., Lazdunski, M., and Borsotto, M. (2002) p11, an annexin II subunit, an auxiliary protein associated with the background K^+ channel, TASK-1. *EMBO J.* **21,** 4439–4448
15. O'Kelly, I., Butler, M. H., Zilberberg, N., and Goldstein, S. A. (2002) Forward transport. 14-3-3 binding overcomes retention in endoplasmic reticulum by dibasic signals. *Cell* **111,** 577–588

16. Renigunta, V., Yuan, H., Zuzarte, M., Rinné, S., Koch, A., Wischmeyer, E., Schlichthörl, G., Gao, Y., Karschin, A., Jacob, R., Schwappach, B., Daut, J., and Preisig-Müller, R. (2006) The retention factor p11 confers an endoplasmic reticulum-localization signal to the potassium channel TASK-1. *Traffic* **7,** 168–181
17. Zuzarte, M., Heusser, K., Renigunta, V., Schlichthörl, G., Rinné, S., Wischmeyer, E., Daut, J., Schwappach, B., and Preisig-Müller, R. (2009) Intracellular traffic of the K^+ channels TASK-1 and TASK-3. Role of N- and C-terminal sorting signals and interaction with 14–3-3 proteins. *J. Physiol.* **587,** 929–952
18. Chatelain, F. C., Bichet, D., Douguet, D., Feliciangeli, S., Bendahhou, S., Reichold, M., Warth, R., Barhanin, J., and Lesage, F. (2012) TWIK1, a unique background channel with variable ion selectivity. *Proc. Natl. Acad. Sci. U.S.A.* **109,** 5499–5504
19. Decressac, S., Franco, M., Bendahhou, S., Warth, R., Knauer, S., Barhanin, J., Lazdunski, M., and Lesage, F. (2004) ARF6-dependent interaction of the TWIK1 K^+ channel with EFA6, a GDP/GTP exchange factor for ARF6. *EMBO Rep.* **5,** 1171–1175
20. Feliciangeli, S., Tardy, M. P., Sandoz, G., Chatelain, F. C., Warth, R., Barhanin, J., Bendahhou, S., and Lesage, F. (2010) Potassium channel silencing by constitutive endocytosis and intracellular sequestration. *J. Biol. Chem.* **285,** 4798–4805
21. Sandoz, G., Thümmler, S., Duprat, F., Feliciangeli, S., Vinh, J., Escoubas, P., Guy, N., Lazdunski, M., and Lesage, F. (2006) AKAP150, a switch to convert mechano-, pH- and arachidonic acid-sensitive TREK K^+ channels into open leak channels. *EMBO J.* **25,** 5864–5872
22. Aldemir, H., Prod'homme, V., Dumaurier, M. J., Retiere, C., Poupon, G., Cazareth, J., Bihl, F., and Braud, V. M. (2005) Cutting edge. Lectin-like transcript 1 is a ligand for the CD161 receptor. *J. Immunol.* **175,** 7791–7795
23. Duprat, F., Lesage, F., Fink, M., Reyes, R., Heurteaux, C., and Lazdunski, M. (1997) TASK, a human background K^+ channel to sense external pH variations near physiological pH. *EMBO J.* **16,** 5464–5471
24. Sandoz, G., Douguet, D., Chatelain, F., Lazdunski, M., and Lesage, F. (2009) Extracellular acidification exerts opposite actions on TREK1 and TREK2 potassium channels via a single conserved histidine residue. *Proc. Natl. Acad. Sci. U.S.A.* **106,** 14628–14633
25. Margeta-Mitrovic, M., Jan, Y. N., and Jan, L. Y. (2000) A trafficking checkpoint controls GABA(B) receptor heterodimerization. *Neuron* **27,** 97–106
26. Ren, Z., Riley, N. J., Garcia, E. P., Sanders, J. M., Swanson, G. T., and Marshall, J. (2003) Multiple trafficking signals regulate kainate receptor KA2 subunit surface expression. *J. Neurosci.* **23,** 6608–6616
27. Standley, S., Roche, K. W., McCallum, J., Sans, N., and Wenthold, R. J. (2000) PDZ domain suppression of an ER retention signal in NMDA receptor NR1 splice variants. *Neuron* **28,** 887–898
28. Bichet, D., Cornet, V., Geib, S., Carlier, E., Volsen, S., Hoshi, T., Mori, Y., and De Waard, M. (2000) The I-II loop of the Ca^{2+} channel α1 subunit contains an endoplasmic reticulum retention signal antagonized by the β subunit. *Neuron* **25,** 177–190
29. Scott, D. B., Blanpied, T. A., Swanson, G. T., Zhang, C., and Ehlers, M. D. (2001) An NMDA receptor ER retention signal regulated by phosphorylation and alternative splicing. *J. Neurosci.* **21,** 3063–3072
30. Garrido, J. J., Giraud, P., Carlier, E., Fernandes, F., Moussif, A., Fache, M. P., Debanne, D., and Dargent, B. (2003) A targeting motif involved in sodium channel clustering at the axonal initial segment. *Science* **300,** 2091–2094
31. Gnad, F., Gunawardena, J., and Mann, M. (2011) PHOSIDA 2011. The posttranslational modification database. *Nucleic Acids Res.* **39,** D253–D260
32. Olsen, J. V., Blagoev, B., Gnad, F., Macek, B., Kumar, C., Mortensen, P., and Mann, M. (2006) Global, *in vivo*, and site-specific phosphorylation dynamics in signaling networks. *Cell* **127,** 635–648
33. Labro, A. J., Raes, A. L., and Snyders, D. J. (2005) Coupling of voltage sensing to channel opening reflects intrasubunit interactions in Kv channels. *J. Gen. Physiol.* **125,** 71–80
34. Long, S. B., Campbell, E. B., and Mackinnon, R. (2005) Voltage sensor of Kv1.2. Structural basis of electromechanical coupling. *Science* **309,** 903–908
35. Bichet, D., Haass, F. A., and Jan, L. Y. (2003) Merging functional studies with structures of inward-rectifier K^+ channels. *Nat. Rev. Neurosci.* **4,** 957–967
36. Kuo, A., Gulbis, J. M., Antcliff, J. F., Rahman, T., Lowe, E. D., Zimmer, J., Cuthbertson, J., Ashcroft, F. M., Ezaki, T., and Doyle, D. A. (2003) Crystal structure of the potassium channel KirBac1.1 in the closed state. *Science* **300,** 1922–1926
37. Ben-Abu, Y., Zhou, Y., Zilberberg, N., and Yifrach, O. (2009) Inverse coupling in leak and voltage-activated K^+ channel gates underlies distinct roles in electrical signaling. *Nat. Struct. Mol. Biol.* **16,** 71–79
38. Bichet, D., Lin, Y. F., Ibarra, C. A., Huang, C. S., Yi, B. A., Jan, Y. N., and Jan, L. Y. (2004) Evolving potassium channels by means of yeast selection reveals structural elements important for selectivity. *Proc. Natl. Acad. Sci. U.S.A.* **101,** 4441–4446
39. Nimigean, C. M., Chappie, J. S., and Miller, C. (2003) Electrostatic tuning of ion conductance in potassium channels. *Biochemistry* **42,** 9263–9268
40. Mathie, A., Rees, K. A., El Hachmane, M. F., and Veale, E. L. (2010) Trafficking of neuronal two pore domain potassium channels. *Curr. Neuropharmacol.* **8,** 276–286
41. Michelsen, K., Yuan, H., and Schwappach, B. (2005) Hide and run. Arginine-based endoplasmic-reticulum-sorting motifs in the assembly of heteromultimeric membrane proteins. *EMBO Rep.* **6,** 717–722
42. Scott, D. B., Blanpied, T. A., and Ehlers, M. D. (2003) Coordinated PKA and PKC phosphorylation suppresses RXR-mediated ER retention and regulates the surface delivery of NMDA receptors. *Neuropharmacology* **45,** 755–767
43. O'Connell, A. D., Leng, Q., Dong, K., MacGregor, G. G., Giebisch, G., and Hebert, S. C. (2005) Phosphorylation-regulated endoplasmic reticulum retention signal in the renal outer-medullary K^+ channel (ROMK). *Proc. Natl. Acad. Sci. U.S.A.* **102,** 9954–9959
44. Mant, A., Elliott, D., Eyers, P. A., and O'Kelly, I. M. (2011) Protein kinase A is central for forward transport of two-pore domain potassium channels K2P3.1 and K2P9.1. *J. Biol. Chem.* **286,** 14110–14119
45. Theilig, F., Goranova, I., Hirsch, J. R., Wieske, M., Unsal, S., Bachmann, S., Veh, R. W., and Derst, C. (2008) Cellular localization of THIK-1 (K(2P)13.1) and THIK-2 (K(2P)12.1) K channels in the mammalian kidney. *Cell Physiol. Biochem.* **21,** 63–74
46. Campanucci, V. A., Fearon, I. M., and Nurse, C. A. (2003) A novel O_2-sensing mechanism in rat glossopharyngeal neurones mediated by a halothane-inhibitable background K^+ conductance. *J. Physiol.* **548,** 731–743
47. Kang, D., Hogan, J. O., and Kim, D. (2013) THIK-1 (K13.1) is a small-conductance background K channel in rat trigeminal ganglion neurons. *Pfluegers Arch.* 10.1007/s00424-013-1358-1
48. Lazarenko, R. M., Fortuna, M. G., Shi, Y., Mulkey, D. K., Takakura, A. C., Moreira, T. S., Guyenet, P. G., and Bayliss, D. A. (2010) Anesthetic activation of central respiratory chemoreceptor neurons involves inhibition of a THIK-1-like background K^+ current. *J. Neurosci.* **30,** 9324–9334
49. Marsh, B., Acosta, C., Djouhri, L., and Lawson, S. N. (2012) Leak K^+ channel mRNAs in dorsal root ganglia. Relation to inflammation and spontaneous pain behaviour. *Mol. Cell Neurosci.* **49,** 375–386